Electrical characterization and modeling of the $Au/CaF_2/n$Si(111) structures with high-quality tunnel-thin fluoride layer

M. I. Vexler,[1,2,a)] N. S. Sokolov,[2] S. M. Suturin,[2] A. G. Banshchikov,[2] S. E. Tyaginov,[2,3] and T. Grasser[3]
[1]Institut für Elektronische Bauelemente und Schaltungstechnik, TU Braunschweig, Hans-Sommer-Straße 66, D-38106 Braunschweig, Germany
[2]A. F. Ioffe Physical-Technical Institute of the Russian Academy of Sciences, 26 Polytechnicheskaya Str., 194021 St.-Petersburg, Russia
[3]Christian-Dopper-Laboratory and Institut für Mikroelektronik, TU Wien, Gußhausstraße 25-29, A-1040 Vienna, Austria

(Received 19 December 2008; accepted 25 February 2009; published online 23 April 2009)

$Au/CaF_2/n$Si(111) structures with 4–5 monolayers of epitaxial fluoride are fabricated and electrically tested. The leakage current in these structures was substantially smaller than in similar samples reported previously. Simulations adopting a Franz-type dispersion relation with Franz mass of $m_F \sim 1.2m_0$ for carriers in the forbidden band of CaF_2 reproduced the measured current-voltage curves quite satisfactorily. Roughly, these curves could also be reproduced using the parabolic dispersion law with the electron mass of $m_e = 1.0m_0$, which is a material constant rather than a fitting parameter. Experimental facts and their comparison to modeling results allow qualification of the crystalline quality of fabricated structures as sufficient for device applications. © *2009 American Institute of Physics*. [DOI: 10.1063/1.3110066]

I. INTRODUCTION

Calcium fluoride—CaF_2—is a promising material for ultrathin dielectric films in silicon electronics.[1] Potentially, there are two major application areas for 1–2 nm fluorides. First, they may be employed in diverse heterostructure devices like resonant-tunneling diodes[2] or CaF_2/CdF_2 superlattices,[3] acting as barrier layers, the whole device being fabricated on a silicon wafer. Second, and perhaps even more important, CaF_2 is a real candidate for gate insulator in field-effect transistors.[4]

Both these perspectives rely on the good dielectric properties of the fluorite,[1] comparable to those of the conventional silicon dioxide. Indeed, it is characterized by a high relative permittivity ($\varepsilon = 8.43$), a wide forbidden gap (12.1 eV), a high field of breakdown [$\sim 10^7$ V/cm (Ref. 4)], and a very small (0.5%) lattice mismatch with silicon.[5] The discontinuities of the conduction (c-) and valence (v-) bands at the Si/CaF_2 heterointerface are large enough [2.38 eV (Ref. 6) and 8.6 eV, respectively] to warrant blocking properties. Barriers formed at the boundaries with the practical gate metals are also high, e.g., the barrier Au/CaF_2 is 2.63 eV. Further, for application as a gate insulator, calcium fluoride has a low tunneling transparency, due to large electron effective mass ($m_e = 1.0m_0$,[1] in parabolic approximation) and due to some features related to the momentum conservation law,[4,7] which reduces leakage and therefore the standby power consumption[8] of a transistor.

The above features of fluorite as a material were recognized long ago. However, the results of earlier investigations into the structures with CaF_2 were not very inspiring.[9–11] The main problem was that the leakage through these structures was much larger than expected, so that the models could only help understand the behavior of the structures. On the one hand, this state-of-the-art reflected the insufficient technology level, and, on the other side, did not stimulate further more profound theoretical studies. Nevertheless, the more or less successful fabrication of some interesting devices with thin CaF_2 films has still been reported, predominately by Japanese groups (e.g. Ref. 2).

In this work we undertake an attempt to improve the crystalline quality of very thin epitaxial fluoride layers, striving to reduce a leakage. The central point in technology optimization was growth at a relatively low temperature, which resulted in a much better homogeneity of the fabricated films. Also we show the possibility of quantitatively reliable modeling of current-voltage (I-V) characteristics of Au/fluorite/nSi(111) metal-insulator-semiconductor (MIS) systems. The new approach in such a modeling is to adopt a Franz-type dispersion relation[12] while calculating the transmission probability. Below, we first describe the samples, their diagnostics and measurements. Section II is devoted to the presentation of the model for tunneling in the structures with CaF_2 layers. Then follows a comparison of simulated and measured current-voltage characteristics with further discussion, rounded off by the conclusion.

II. SAMPLES: MEASURED CURRENT-VOLTAGE CURVES

In this work, $Au/CaF_2/n$Si(111) MIS structures with 4 and 5 monolayer (ML=3.15 Å) fluoride films were grown, diagnosed by atomic force microscopy (AFM) and electrically tested. These were two-electrode, i.e., diode, samples, called also MIS capacitors, fabricated on low-doped ($N_D = 10^{15}$ cm^{-3}) silicon wafers; the thickness of the top (gate) gold contact exceeded 20 nm.

a)Electronic mail: shulekin@mail.ioffe.ru.

 © 2009 American Institute of Physics

Author complimentary copy. Redistribution subject to AIP license or copyright, see http://jap.aip.org/jap/copyright.jsp

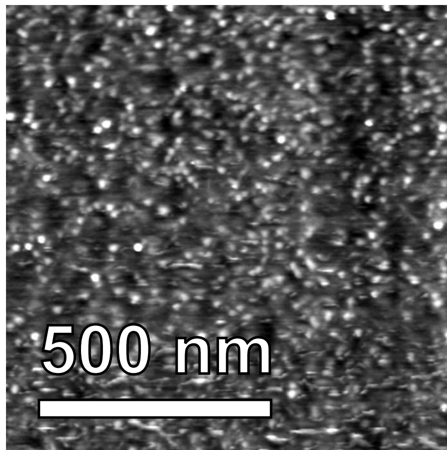

FIG. 1. AFM image of the CaF_2 surface (image size is 1×1 μm^2; the maximal height difference between the black and white points is 2.8 nm).

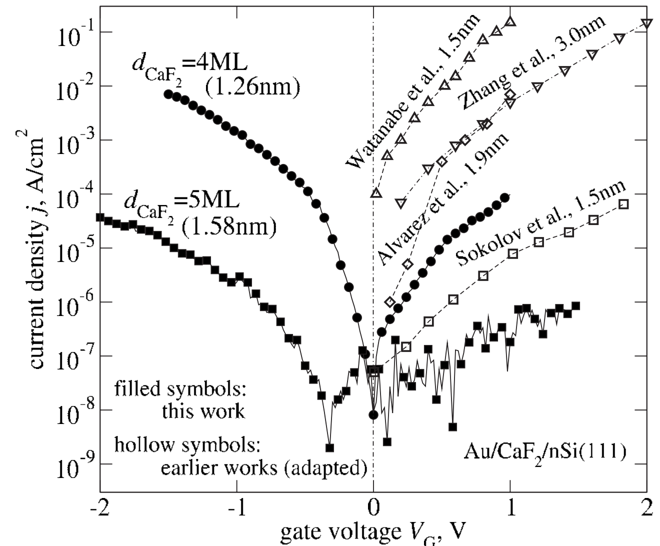

FIG. 2. Measured *I-V* curves of fabricated MIS capacitors, completed by the data of Refs. 4 and 9–11. The lines serve as a guide for eyes.

The most crucial technological step is the formation of the thin CaF_2 layer, which is done by molecular beam epitaxy (MBE). Si wafers with a miscut angle not exceeding 10′ were chemically cleaned[13] and then annealed at 1200 °C for 2 min in ultrahigh vacuum. The MBE process was performed with a deposition rate of 2 ML/min, and controlled by high-energy electron diffraction. It was found that 250 °C is an optimal growth temperature. It is low enough to avoid triangularly shaped pinholes, usual for thin high-temperature CaF_2 layers.[9] On the other hand, it is high enough to provide reasonable crystalline quality of the fluoride film.

Low spatial fluctuation of thickness in these films was confirmed by the AFM images (Fig. 1). The image in Fig. 1 has an enhanced contrast so that the roughness is, in fact, very minor, despite a first impression of warped relief. The estimated AFM height deviation (rms value) lies near 0.1 nm, and the correlation length of thickness fluctuations is about 20 nm. Note that the thicker CaF_2 layers not discussed in this work were characterized by much worse rms parameters.

Within a few minutes after the formation of the insulating film, the circular gold gate contacts ($S=5\times 10^{-5}$ cm^2) were deposited through the mask.

The measurements of the current-voltage characteristics were started soon after the sample fabrication, in order to evade any problems related to a slow parasitic oxidation occurring in an atmospheric ambient and becoming revealable in several days.

For electrical measurements, the AFM-based installation with the gold-coated cantilever has been exploited. This technique allowed for reliable and safe contacting the small-area samples, due to a precise automated tip pressure adjustment. The screening cap of the AFM ensured the noise reduction and the protection from an external light. Static *I-V* curves were recorded using Keithley 2400 SourceMeter, which simultaneously served as a voltage generator and digital ammeter. The measurement process was controlled by a special program providing the remote operation of the SourceMeter. The sensitivity reached 2×10^{-12} A. In order to attain best accuracy, the maximum available internal sampling time of the SourceMeter has been used. Moreover the value of current was sequentially read, for each gate voltage V_G, several times that effectively made the sampling time even larger and also reduced the dynamic capacitance recharge distortions. The measurement voltage range was limited by damage of the structures.

Experimental current-voltage curves, together with the results of some previous works, including our own for inferior samples, are shown in Fig. 2. A positive voltage presumes the application of "+" to the metal electrode. Presently, the current densities are seen to be lower than those in all previous studies. This observation elucidates the improvement of an overall sample quality. Indeed, the superfluous current crowding in thinnest places should vanish with a reduction in the insulator thickness deviation.

Beyond the range of very low voltages, the *I-V* curves (Fig. 2) are nearly exponential. This is typical for MIS structures in accumulation ($V_G>0$) and, with respect to the reverse bias conditions, evidences for the availability of a sufficient amount of minority carriers.[14] There is, further, a pronounced difference between the 4 and 5 ML samples (although the thickness difference is as small as 1 ML). The effect of thickness is here stronger, compared to the MIS structures with a conventional silicon dioxide, due to the substantially larger electron effective mass [$1.0m_0$ in fluoride,[1] versus $0.42m_0$ in SiO_2 (Ref. 14)]; this is also one of the reasons for the relatively low tunnel transparency of CaF_2 layers[4] as already mentioned. It is only somewhat unusual that the reverse currents are 10–30 times larger than the forward ones. However, we will theoretically explain this in the paper. The sample-to-sample deviation of the current density was about half an order of magnitude; such a good reproducibility additionally solidifies the achieved technology level.

III. MODEL BASICS

A. General simulation principles

Our simulations of current-voltage curves rely on the regular theories of MIS tunnel structures.[14–16] For this rea-

Author complimentary copy. Redistribution subject to AIP license or copyright, see http://jap.aip.org/jap/copyright.jsp

son, only the main points are recalled below, emphasizing the aspects especially important for tunneling in calcium fluoride films.

The total current always consists of components provided by carrier transport between metal and Si c-band, j_{cm}, as well as between metal and Si v-band, j_{vm},

$$j = j_{cm} + j_{vm}. \tag{1}$$

We avoid the words "electron/hole currents" because hole tunneling may anyway be interpreted as electron tunneling backward and vice versa.

Under reverse bias condition, i.e., for n-silicon, at $V_G < 0$, the voltage partitioning in a MIS diode is found so that to satisfy the balance equation,

$$j_{vm} = j_{cm} \times (M - 1) + j_d + j_{\mathrm{gen}}, \tag{2}$$

where M is the multiplication factor (=1 in context of this work), j_d is a pn-junction-like current from bulk to inversion layer, and j_{gen} accounts for thermal generation. The two last components normally have the forms

$$j_d = A\left(1 - \exp\frac{E_{Fn} - E_{Fp}}{k_B t}\right), \quad A = \mathrm{const} \tag{3}$$

$$j_{\mathrm{gen}} = q(w - w|_{V_G=0})G \tag{4}$$

with w for the depletion layer width and $E_{Fn|Fp}$ for the electron and hole Fermi energies in Si. In our simulations of MIS tunnel diodes with an oxide layer, the value $G = 10^{23}-10^{24}\ \mathrm{m^{-3}\,s^{-1}}$ was usually taken for the thermal generation rate (e.g. Ref. 16).

Alternatively, one can admit that there is always an equilibrium ($E_{Fn} \approx E_{Fp}$) in silicon. With such an assumption, the voltage partitioning is being found prior to and independently of the currents, and Eq. (2) is void. As will be shown further this simple approach yields partly acceptable results also for the studied structures with CaF_2.

B. Tunneling current calculation

The current flowing through a MIS structure involves the continuum (3D-3D tunneling) and discrete (2D-3D) fractions,

$$j = \frac{4\pi q \nu m_\perp}{h^3}\int\int \Delta_F T(E,E_\perp)dE_\perp dE + \frac{q\nu m_\perp}{\tau_w \pi \hbar^2}\int \Delta_F T(E,|E - E_0|)dE. \tag{5}$$

Here, E denotes the total energy of a carrier and $E_\perp$ denotes the energy of its motion in Si in the interface plane; $m_\perp$ and ν are the effective mass in this plane and the degeneracy factor, τ_w is the aller-retour time for particles on the ground level E_0 of an inversion or accumulation layer, and $\Delta_F = \Delta_F(E)$ is the difference between the Fermi functions in the silicon substrate and in the metal. Integration limits are dictated by the energy and the momentum conservation laws, the continuous term being splitted into c-band- and v-band-associated parts, and the discrete term contributing to j_{cm} or j_{vm} only. The Fermi quasilevel and the values of $m_\perp$ and ν in Si are taken for the relevant carrier type in each case.

Since CaF_2 is a crystalline dielectric, the conservation of a transverse momentum $\vec{k}_\perp$ should be correctly accounted for, namely, one has to consider the large $\perp$ component of electron wave vectors at the c-band minima in Si for the (111) surface,

$$k_{0\perp} = \sqrt{\frac{2}{3}} \times k_0 = \sqrt{\frac{2}{3}} \times \frac{2\pi}{a} \times \delta \tag{6}$$

with lattice constant $a = 5.43$ Å and $\delta \approx 0.85$ (minimum in $2\pi/a$ units). In simulations of tunneling through the amorphous SiO_2, the component $k_{0\perp}$ is often ignored, as if silicon were a direct-band semiconductor, but such an approach seems to be inadequate for calcium fluoride. It is evident and will be further supported by formulae that the transmission probability T for any pair E, $E_\perp$ is much lower than it would have been with $k_{0\perp} = 0$. So, although it may sound unusual, the valence band current j_{vm} is expected to overwhelm the conduction band current j_{cm} in many regimes.

C. Transmission probability: Franz-type dispersion relation

For the transmission probability, the Wentzel–Kramers–Brillouin formula

$$T(E,E_\perp) = \frac{4|v_s||v_i|}{|v_s|^2 + |v_i|^2} \times \exp\left(-2\int |k_z(z)|dz\right) \tag{7}$$

is used where the tunneling-direction component k_z of a wave vector is integrated between classical turning points. The prefactor containing the carrier velocity in z-direction in substrate (s) and insulator[17] smoothes T near the Si band edges.

In a barrier, the k_z component is purely imaginary and its square may be written as

$$k_z^2 = \frac{2m_e}{\hbar^2}\left[E_e - \frac{\hbar^2 k_\perp^2}{2m_e}\right] \tag{8}$$

assuming that the valence band discontinuity is huge and so a tunneling in CaF_2 has one-band character;[18] m_e ($m_e \approx 1.0 m_0$) denotes the electron effective mass in the conduction band of fluoride and $E_e(<0)$ is the particle energy counted from the conduction band edge of insulator and therefore coordinate dependent.

The expression (8) comes from the parabolic dispersion law for carriers in the fluoride. In the absence of exact information on this relation, it is the most natural assumption. However, in our work we shall also examine another variant, known as Franz-type relation, yielding

$$k_z^2 = \frac{2m_F}{\hbar^2}\left[E_e\left(1 + \frac{E_e}{E_{gi}}\right) - \frac{\hbar^2 k_\perp^2}{2m_F}\right]. \tag{9}$$

Here, m_F ($m_F \neq m_e$) is the Franz effective mass and E_{gi} is the band gap of the fluoride. Such expression is known to give better results than the parabolic one, in some cases (e.g. Ref. 19, SiO_2) and, what is also important, allows for avoiding a division of tunneling processes to electron and hole tunnel-

Author complimentary copy. Redistribution subject to AIP license or copyright, see http://jap.aip.org/jap/copyright.jsp

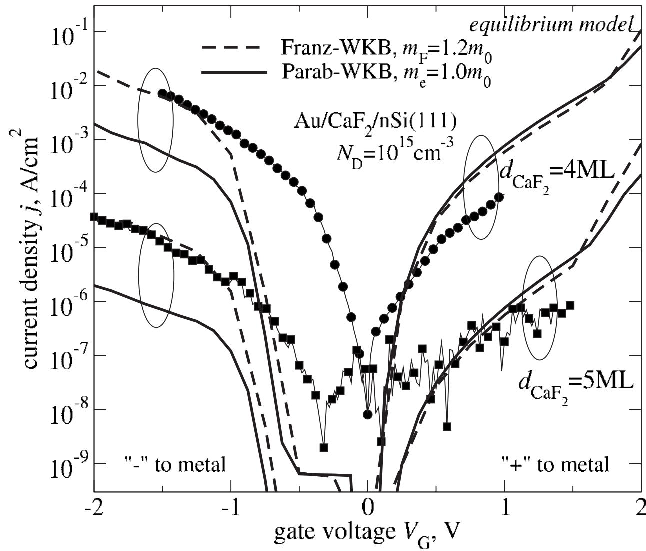

FIG. 3. Measured and with equilibrium approach simulated I-V curves.

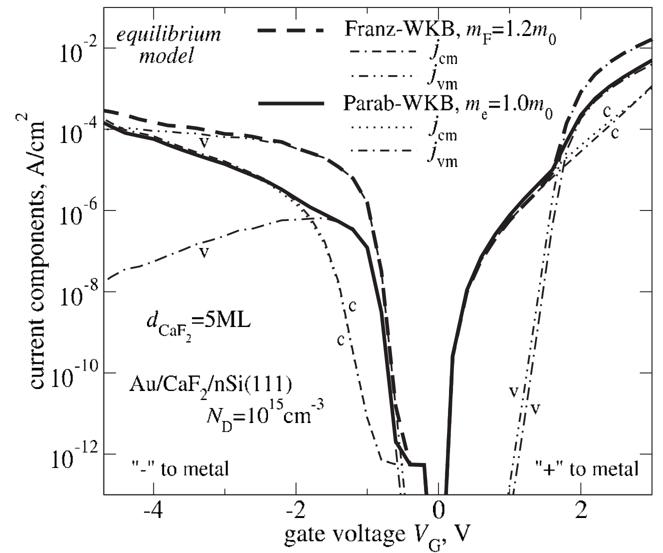

FIG. 4. Individual current components.

ing whose artificity is especially clear with respect to tunneling with energies near the mid of the insulator band gap.

For the sake of simplicity, we write $k_\perp$ as

$$k_\perp^2 = k_{0\perp}^2 + \frac{2m_\perp}{\hbar^2} E_\perp . \tag{10}$$

Fair but much more complicated would be to account for the carrier momentum in the plane; in such a case also Eq. (5) should have been modified. However, the main role belongs anyway to the term $k_{0\perp}^2$.

IV. SIMULATION RESULTS: DISCUSSION

We first show the curves obtained within an assumption of equilibrium for silicon. This is a very frequently used or implied approach.

In Fig. 3, the simulation results are presented together with the experimental data. The negative biases correspond to inversion or depletion, while the positive to the accumulation conditions in the substrate. One pair of curves is generated with the parabolic [expression (8)] and another with Franz-type [Eq. (9)] relation. The Franz mass m_F was set here to $1.2m_0$. That this value appears to be larger than m_e is quite normal and occurs also in other insulators; so in SiO_2, $m_F \sim 0.6m_0$ (Ref. 17) while $m_e = 0.42m_0$.

One can definitively say that the application of Franz dispersion relation allows for obtaining better agreement with the experimental data. Particularly, the asymmetry of the current-voltage characteristics is correctly reproduced. For $V_G \sim -2$ V the numeric coincidence is almost ideal, for positive biases it is also not bad. Note that variations in the effective mass m_e in the parabolic relation would not help because either the positive or the negative branch would be fitted even worse than with $m_e = 1.0m_0$. The crucial feature of the Franz relation arises from the fact that this relation implies the reduction in the electron mass while departing from the band edges toward the middle of the gap of an insulator. So, the calculated current between the metal and the valence band of Si becomes larger, while the conduction band current remains unchanged.

Figure 4 shows the separately simulated current components. We see the competition of the valence-band and conduction-band currents. j_{vm} is comparable to j_{cm} because the necessity of the transversal momentum conservation reduces the barrier transparency for tunneling from the conduction band. Only at low positive voltages V_G when the valence-band transport is blocked due to the band bending in Si, the electron component j_{cm} flows alone. It is worth to mention also the remarkable behavior of the j_{vm} component under negative biases. In the parabolic model, since the averaged barrier height for the valence band tunneling increases with voltage (one-band transport), j_{vm} exhibits a maximum and then decreases for higher $|V_G|$. Within the Franz model, no pronounced decrease is seen, but there is an apparent slowdown of j_{vm} of the same origin.

A plateau at low negative voltages predicted by simulations (Figs. 3 and 4) is quite typical for MIS structures on low-doped substrates and appears also for more conventional devices with SiO_2.[20] However it is not observed for our $Au/CaF_2/nSi$ samples.

Now we should analyze how adequate is the equilibrium model for the studied structures at $V_G < 0$. For this purpose and also in order to understand the origin of the discrepancy near zero, we performed simulations using the MIS tunnel diode model based on Eq. (2). The equilibrium case can be imitated with this model by taking some very large A and $j_{gen} \approx 0$ in Eqs. (3) and (4). Then the hole Fermi quasilevel E_{Fp} lies just a little bit above E_{Fn} and the current j_d warrants the tunnel hole leakage.

However, while j_d and j_{gen} are set to their usual values, particularly G to 10^{23} m^{-1} s^{-1}, we get current saturation (Fig. 5) due to the lack of minority carriers resulting in $E_{Fp} \gg E_{Fn}$ at high bias $|V_G|$. Simultaneously at low voltages, E_{Fp} is placed beneath E_{Fn} and the current increases, as the

Author complimentary copy. Redistribution subject to AIP license or copyright, see http://jap.aip.org/jap/copyright.jsp

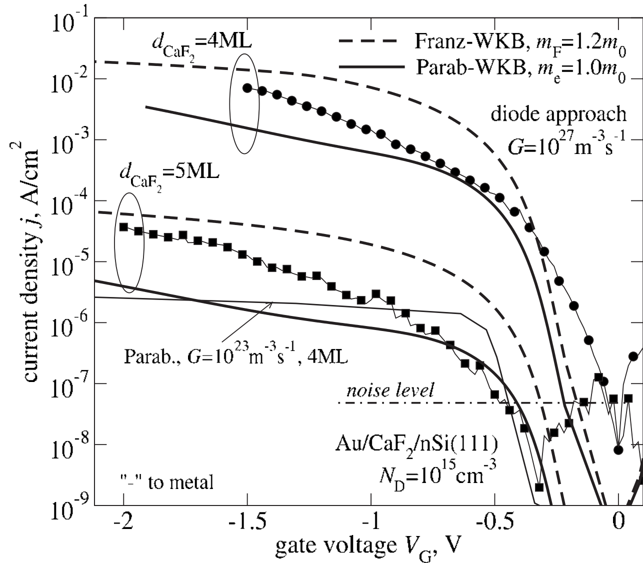

FIG. 5. Measured and simulated within diode approach *I-V* curves, reverse bias. Excessive minority carrier generation is additionally assumed.

minority carrier supply in this regime is excessive, compared to that required to support equilibrium. The problem of hole deficiency can be numerically avoided, even in a 4 ML sample, augmenting the thermal generation rate e.g., to $G=10^{27}$ m^{-1} s^{-1}. Then the experimental data are reproduced throughout the whole voltage range. The abnormal G value implies the presence of a great amount of defects in silicon near the CaF_2 interface, which is not so unlikely.

In this context, a trend toward reduction in a current with time[18] should be mentioned. Probably, the defects responsible for the large generation rate are being gradually relaxed ("interface formation") and G drops to its ordinary level. Independently of that, the deterioration of the CaF_2 film at high electric loads enables an electron transport violating the tunnel models, particularly the conservation laws, and also makes the hole supply insufficient for the same insulator voltage as in a fresh structure. Studies of a fluoride layer degradation[18] reveal a complex picture of current evolution due to interplay of j_{cm} and j_{vm}. At the initial stage, additionally to the schema of Ref. 18, the relaxation of a defect-mediated thermal generation is now supposed to reduce j_{vm} and the insulator voltage. Such a stage is less critical in MIS capacitors with thicker (e.g., 6 ML) fluorides where the demand on holes is less and j_{cm} may become more important.

Note that the equilibrium approach for the reverse bias gives an estimation of nearly maximal current attainable at relatively large $|V_G|$. The reserve on current increase due to even extreme intrinsic generation is restricted, except near $V_G=0$.

The results obtained with the parabolic dispersion law, despite a not very good agreement to the experiment, are still useful. Namely, we can claim that the measured currents roughly correspond to the theoretical prediction with a mass of m_0 for electrons and not with a much lower mass value. This is a direct confirmation of the good insulating quality of studied CaF_2 layers. Indeed, the value of $1.0m_0$ agrees with the fact of large separation between the valence and conduction bands of fluoride, while the necessity to adopt smaller values would have meant that the film behavior contradicts its band structure.

V. CONCLUSION

The synopsis of this work can be formulated as follows:

- Fabricated Au/(4–5 ML)CaF_2/nSi(111) samples exhibit superior electrical characteristics, especially lower leakage, compared to previously reported results.
- Transverse momentum of electrons tunneling through thin CaF_2 film is conserved, *I-V* curves are approximately repeated by simulations using a one-band insulator model with an independently known effective mass value $m_e=1.0m_0$.
- Adoption of a Franz-type dispersion law for calcium fluoride, with $m_F\sim 1.2m_0$, allows us to get good quantitative agreement with the measurements, particularly to explain the asymmetry of the experimental *I-V* characteristics.
- There evidently flows an excessive current under low negative bias at the metal, which probably arises due to the stronger thermal generation in silicon and at the CaF_2/Si interface, compared to similar structures with silicon dioxide.

In general, the results of this study allow a more optimistic look in the future of thin fluoride barrier layers and the hope that they may find application in diverse silicon-based electron devices.

ACKNOWLEDGMENTS

The authors appreciate partial support of this work by Russian Foundation for Basic Research (Grant No. 07-02-0900) and by FWF (Project No. 18316-N13) as well as stimulating discussions with Professor K. Saiki and Dr. S. Ikeda at early stage of this study.

[1] *Crystals with the Fluorite Structure: Electronic, Vibrational, and Defect Properties*, edited by W. Hayes (Clarendon Press, Oxford, 1974).
[2] M. Watanabe, Y. Iketani, and M. Asada, Jpn. J. Appl. Phys., Part 2 **39**, L964 (2000).
[3] A. Yu. Khilko, S. V. Gastev, R. N. Kyutt, M. V. Zamoryanskaya, and N. S. Sokolov, Appl. Surf. Sci. **123–124**, 595 (1998).
[4] N. S. Sokolov, I. V. Grekhov, S. Ikeda, A. K. Kaveev, A. V. Krupin, K. Saiki, K. Tsutsui, S. E. Tyaginov, and M. I. Vexler, Microelectron. Eng. **84**, 2247 (2007).
[5] N. S. Sokolov, N. L. Yakovlev, and J. Almeida, Solid State Commun. **76**, 883 (1990).
[6] Ph. Avouris and R. Wolkow, Appl. Phys. Lett. **55**, 1074 (1989).
[7] C. Strahberger and P. Vogl, Phys. Rev. B **62**, 7289 (2000).
[8] J. D. Plummer and P. B. Griffin, Proc. IEEE **89**, 240 (2001).
[9] S. Watanabe, M. Maeda, T. Sugisaki, and K. Tsutsui, Jpn. J. Appl. Phys., Part 1 **44**, 2637 (2005).
[10] B. Zhang, K. Furuya, Y. Ikeda, and N. Kikegawa, Jpn. J. Appl. Phys., Part 1 **38**, 4887 (1999).
[11] J. C. Alvarez, M. I. Vexler, I. V. Grekhov, N. S. Sokolov, and A. F. Shulekin, Semiconductors **30**, 698 (1996) (translated from Russian).
[12] W. Franz, in *Handbuch der Physik*, edited by S. Flügge (Springer, Berlin, 1956), Vol. 18, p. 155.
[13] A. Ishizaka and Y. Shiraki, J. Electrochem. Soc. **133**, 666 (1986).

Author complimentary copy. Redistribution subject to AIP license or copyright, see http://jap.aip.org/jap/copyright.jsp

[14]A. Schenk and G. Heiser, J. Appl. Phys. **81**, 7900 (1997).
[15]Z. A. Weinberg, Solid-State Electron. **20**, 11 (1977).
[16]S. E. Tyaginov, M. I. Vexler, A. F. Shulekin, and I. V. Grekhov, Microelectron. Eng. **83**, 376 (2006).
[17]L. F. Register, E. Rosenbaum, and K. Yang, Appl. Phys. Lett. **74**, 457 (1999).
[18]M. I. Vexler, S. M. Suturin, S. E. Tyaginov, A. G. Banshchikov, and N. S. Sokolov, Thin Solid Films **516**, 8740 (2008).
[19]Y. T. Hou, M. F. Li, Y. Jin, and W. F. Lai, J. Appl. Phys. **91**, 258 (2002).
[20]T. Yoshimoto and K. Suzuki, Jpn. J. Appl. Phys., Part 2 **32**, L180 (1993).

Author complimentary copy. Redistribution subject to AIP license or copyright, see http://jap.aip.org/jap/copyright.jsp